Journal of Bone Oncology 2 (2013) 95–104

Contents lists available at ScienceDirect

Journal of Bone Oncology

journal homepage: www.elsevier.com/locate/jbo

Research Article

Osteoprotegerin inhibits bone resorption and prevents tumor development in a xenogenic model of Ewing's sarcoma by inhibiting RANKL

Gaëlle Picarda [a,b], Etienne Matous [a,b], Jérôme Amiaud [a,b], Céline Charrier [a,b], François Lamoureux [a,b], Marie-Françoise Heymann [a,b,c], Franck Tirode [d], Bruno Pitard [e], Valérie Trichet [a,b], Dominique Heymann [a,b], Françoise Redini [a,b,*]

[a] INSERM, Equipe Ligue Contre le Cancer 2012, UMR-957, Nantes F-44035, France
[b] Université de Nantes, EA3822, Faculté de Médecine, Laboratoire de physiopathologie de la résorption osseuse et thérapie des tumeurs osseuses primitives, Nantes F-44035, France
[c] Service d'anatomo-pathologie, CHU Hôtel Dieu, Nantes F-44035, France
[d] INSERM UMR830, Institut Curie, 26 rue d'Ulm, Paris F-75006, France
[e] INSERM UMR1087, IRT-UN, Quai Moncousu, Nantes F-44035, France

ARTICLE INFO

Article history:
Received 22 March 2013
Received in revised form
29 April 2013
Accepted 29 April 2013
Available online 20 May 2013

Keywords: Ewing's sarcoma
Osteoprotegerin
RANKL
Bone resorption
TRAIL

ABSTRACT

Ewing's sarcoma (ES) associated with high osyeolytic lesions typically arises in the bones of children and adolescents. The development of multi-disciplinary therapy has increased current long-term survival rates to greater than 50% but only 20% for high risk group patients (relapse, metastases, *etc.*). Among new therapeutic approaches, osteoprotegerin (OPG), an anti-bone resorption molecule may represent a promising candidate to inhibit RANKL-mediated osteolytic component of ES and consequently to limit the tumor development.

Xenogenic orthotopic models of Ewing's sarcoma were induced by intra-osseous injection of human TC-71 ES cells. OPG was administered *in vivo* by non-viral gene transfer using an amphiphilic non ionic block copolymer. ES bearing mice were assigned to controls (no treatment, synthetic vector alone or F68/empty pcDNA3.1 plasmid) and hOPG treated groups. A substantial but not significant inhibition of tumor development was observed in the hOPG group as compared to control groups. Marked bone lesions were revealed by micro-computed tomography analyses in control groups whereas a normal bone micro-architecture was preserved in the hOPG treated group. RANKL over-expressed in ES animal model was expressed by tumor cells rather than by host cells. However, TRAIL present in the tumor microenvironment may interfere with OPG effect on tumor development and bone remodeling via RANKL inhibition.

In conclusion, the use of a xenogenic model of Ewing's sarcoma allowed discriminating between the tumor and host cells responsible for the elevation of RANKL production observed in this tumor and demonstrated the relevance of blocking RANKL by OPG as a promising therapy in ES.

1. Introduction

Ewing's sarcoma (ES) is a high-grade neoplasm representing the second most common primary bone malignancy in both children and adults. With a peak incidence at 15 years, this disease accounts for 2% of childhood cancers [1–3]. ES is defined as a bone tumor which may occur at any site within the skeleton but preferentially affects the trunk and the diaphysis of long bones. Less commonly, it arises in extraskeletal soft tissues (15%). It is characterized by a rapid tumor growth and extensive bone destruction that can result in bone pain and pathological fracture. A particularity of ES tumors is the occurrence of a typical chromosomal translocation that fuses the EWS gene on chromosome 22q12 to a member of the ETS transcription gene family, most commonly to Fli-1 on 11q24 (> 90% of cases) [4,5]. This translocation leads to the production of an aberrant transcription factor that promotes tumorigenicity [6–8]. Due to progress in surgery and chemotherapy, survival rates have increased from less than 10% to 55–60% for patients presenting local disease [9]. However, the survival rates decrease to 15–25% when metastases are detected at diagnosis, or for patient presenting resistance to treatment or relapsed disease. Moreover, a survival plateau seems to have been reached with conventional therapies. Accordingly, new therapeutic approaches should be actively explored, especially for high-risk patients, to increase long-term survival by

* Correspondence to: INSERM UMR957, Faculté de Médecine, 1 rue Gaston Veil, 44 035 Nantes Cedex 1, France. Tel.: +33 240 412842; fax: +33 240 412860.
E-mail address: francoise.redini@univ-nantes.fr (F. Redini).

2212-1374/$ - see front matter © 2013 Elsevier GmbH. This is an open access article under the CC BY-NC-ND license (http://creativecommons.org/licenses/by-nc-nd/4.0/).
http://dx.doi.org/10.1016/j.jbo.2013.04.004

decreasing metastases development and preventing drug resistance.

ES is characterized by extensive bone destruction due to osteolysis. Ewing's sarcoma cells are unable to directly degrade the bone matrix and accordingly, osteoclast activation and subsequent bone resorption might be responsible for the clinical features of bone destruction [10]. Indeed, as demonstrated for bone metastases [11], a vicious cycle between bone cells (osteoclasts and osteoblasts) and tumor cells occurs during the development of tumor in bone site. Therefore, targeting the osteoclasts may represent a promising adjuvant strategy for the treatment of bone tumors. Among the factors involved in the regulation of bone remodeling, the molecular triad osteoprotegerin (OPG)/receptor activator of NF-kB (RANK)/RANK Ligand (RANKL) is strongly implicated [12,13]. Osteoclast differentiation and activation is mainly mediated by RANKL, a cytokine member of the tumor necrosis factor (TNF) superfamily (TNFSF11) that binds to its receptor RANK at the surface of osteoclasts [14]. OPG (TNFRSF11B) is a soluble protein that acts as a decoy receptor for RANKL inhibiting osteoclast formation, function and survival by preventing the binding of RANKL to RANK [15]. Transgenic mice overexpressing OPG exhibit an osteopetrotic phenotype, whereas OPG-knockout mice have severe osteoporosis [16,17]. The OPG/RANKL/RANK system is also involved in various pathologies associated with tumors in bone [18,19]. Therefore, OPG has demonstrated increased interest as a therapeutic strategy in malignant bone pathologies associated with osteolytic lesions [20,21]. Concerning primary bone tumors, the inhibition of RANKL activity by OPG induced a significant therapeutic effect on bone lesion and tumor development in two preclinical models of osteosarcoma in mice (POS-1) and in rats (OSRGa) [22]. This effect was also confirmed by using the soluble form of the RANKL receptor, RANK-Fc [15] or by the RNA interference strategy targeting RANKL [23]. In addition, OPG is also able to bind to the TNF Related Apoptosis Inducing Ligand (TRAIL), another member of the TNF superfamily (TNFSF10) [23], thereby limiting its ability to induce apoptosis in tumor cells. It has been even reported that OPG acts as a pro-tumoral factor in some cancer cell lines *in vitro* [24–26]. In addition, Taylor et al. previously reported that the expression of RANKL in Ewing's sarcoma cell lines and tissues could support osteoclast activation [10]. Therefore, targeting this cytokine with OPG may represent a promising therapeutic option.

The aim of this study was to determine the therapeutic relevance of blocking RANKL in Ewing's sarcoma by using OPG administered by non-viral gene transfer approaches in two models of human Ewing sarcoma in immunodeficient mice. OPG was administered using amphiphilic polymers constituted by blocks of poly(ethylene oxide) and of poly(propylene oxide) as previously reported for osteosarcoma preclinical studies [22]. These synthetic vectors have been used with high efficiency for *in vivo* gene transfer in various organs including skeletal and cardiac muscles [27,28] and in lungs [29]. Intramuscular injections of these synthetic vectors led to the synthesis of proteins for local benefit such as dystrophin or of systemic erythropoietin [30].

2. Materials and methods

2.1. In vivo experiments

2.1.1. Plasmid constructs

The pcDNA3.1.3-hOPG1-194 contains the cDNA coding for the truncated form of OPG (1–194) cloned using the pcDNA™ 3.3-TOPO® TA cloning® Kit (Invitrogen) according to manufacturer's recommendations, the empty pcDNA3.1 plasmid (Invitrogen) being used as a control.

2.1.2. Xenograft models of human Ewing's sarcoma

All procedures involving mice were conducted in accordance with the institutional guidelines of the French Ethical Committee (CEEA.PdL.06, protocol number 2010.23). Four-week-old male athymic mice purchased from Harlan were housed in the Experimental Therapeutic Unit at the Faculty of Medicine of Nantes (France). The TC-71 ES model was induced by transplantation of a fragment of tumor ($2 \times 2 \times 2$ mm^3) in close contact with the tibia, resulting from the initial injection of 2×10^6 TC-71 ES cells next to the tibia. To confirm the effects of OPG, another Ewing's sarcoma model was developed, induced by i.m. injection of 2×10^6 human A-673 ES cells in close contact with the tibia, leading to a rapidly growing tumor in soft tissue with secondary contiguous bone invasion. Mice were anesthetized by inhalation of a combination of isoflurane/air (1.5%, 1 L/min) and buprenorphine was given by sc injection during the protocol (0.05 mg/kg; Temgesic®, Schering-Plough).

2.1.3. Synthetic gene transfer

The synthetic vector used in this study (named F68) belongs to the Lutrol family of vectors, non ionic block copolymers of poly (ethyleneoxide)$_{75}$-poly(propyleneoxide)$_{30}$-poly(ethyleneoxide)$_{75}$ generously provided by Dr. Bruno Pitard (INSERM UMR1087, Nantes, France) [30]. Stock solutions were prepared at 6% (w/v) in water and stored at 4 °C. Formulations of DNA with block copolymers were prepared by equivolumetric mixing block copolymers in water and DNA solution at the desired concentration (50 μg/muscle).

2.1.4. Experimental protocol

Groups of 6–8 mice were assigned as control vectors (F68/pcDNA3.1 alone) and hOPG1-194 (F68/pcDNA3.1-OPG1-194). F68 alone or associated with the empty vector pcDNA3.1 does not affect tumor development as compared to non-treated mice that develop the Ewing sarcoma model (data not shown). Mice were anesthetized by inhalation of a combination of isoflurane/air (1.5%, 1 L/min) and the F68/DNA formulations were injected into both tibial anterior muscles once a week. Because the transgene expression is optimal seven days after injection of the DNA formulations, the treatment began 7 days before Ewing's sarcoma implantation as a preventive treatment, up to 21 days post-implantation. The truncated form of OPG was chosen in accordance to previous results obtained by our group in osteosarcoma models, showing that the biological activity of the complete OPG isoform may be limited by interaction with proteoglycans present in the extracellular matrix, inhibiting OPG biological availability [31]. The Ewing sarcoma model was induced by tumor fragment transplantation or tumor cell injection as described above. The tumor volume was calculated by using the formula $L \times l^2/2$, where L and l are the longest and the smallest perpendicular diameter, respectively. Treatment continued until each animal showed signs of morbidity, which included cachexia or respiratory distress, at which point they were sacrificed by cervical dislocation or by CO_2 inhalation. The mice were also sacrificed for ethical reasons when the tumor volume exceeded 3000 mm^3. Lung tumor dissemination was assessed at necropsy. The tumor-bearing hind limb was dissected and kept in 10% paraformaldehyde for radiography, micro-computed tomography (micro-CT) and histological analyses.

2.1.5. Micro-computed tomography (micro-CT) analysis

Analyses of bone micro-architecture were performed using a Skyscan 1076 *in vivo* micro-CT scanner (Skyscan, Kontich, Belgium). Tests were performed after sacrifice on tibias for each treatment group. All tibias were scanned using the same parameters (pixel size 18 μm, 50 kV, 0.5-mm Al filter, 10 min of scanning).

The reconstruction was analyzed using NRecon and CTan software (Skyscan). The specific bone volume was quantified as the relative Bone volume/total volume measured for each VOI. 3D visualizations of tibias and heads were realized using ANT software (Skyscan) at sacrifice.

2.1.6. In vivo analysis of transgene expression

Blood was drawn intermittently from the retro-orbital vein to monitor circulating hOPG protein levels throughout the experiment. At necropsy, the tumor tissues were lysed in Reporter Lysis Buffer (Promega, Madison, USA) supplemented with a protease inhibitor cocktail (Roche Molecular Biomedicals, Manheim, Germany), and crushed during 30 s using Ultraturax®, after which lysates were centrifuged at 10,000 rpm for 5 min at 4 °C, and processed for hOPG detection using ELISA kit (R&D Systems) following the manufacturer's recommendations.

2.1.7. RANKL immuno-fluorescence on animal tumor models

After sacrifice, tumor samples were fixed in a solution of paraformaldehyde (PFA) 4% at 4 °C for. The samples were then cryopreserved consecutively in 6% and 30% sucrose solutions in PBS pH 7.4 buffer. They were then embedded in Neg50 (Thermo-Scientific) and frozen in isopentane cooled to −80 °C. The 40 μm cryostat sections (also named floating sections) were then collected in well plates in 1 × PBS, 0.1% Thimerosal pH=7.4 and stored at 4 °C. Sections were then washed 3 times for 5 min in 1 × PBS. Permeabilization is then performed with 1 × PBS, 0.1% Triton 100 ×. The sections were then washed 3 times for 5 min in a solution of 1 × PBS. The unspecific sites were first blocked by incubating the sections for 25 min in blocking solution 1 [1 × PBS containing 5% goat serum (Dako) and 1% BSA (Sigma)] followed by endogenous immunoglobulins quenching during 1 h in the blocking solution 2 [Fab fragments of goat antibodies directed against mouse (Jackson Lab) diluted 1/10 in PBS 1 ×]. The sections were then incubated overnight at 4 °C with the primary antibody targeting human RANKL (R&D) diluted 1/20 in blocking solution 3 [1 × PBS containing 5% rabbit serum (Jackson Lab) and 1% BSA]. They are then washed 3 times for 5 min in a 1 × PBS and then incubated for 45 min with the secondary rabbit antibody directed against goat IgG [Life Technologies] diluted 1/200 in blocking solution 3. The sections were mounted between slides and coverslips using Moviol (Sigma), stored at 4 °C in the dark before being analyzed by confocal microscopy (imaging platform MicroPicell, SFR26, Nantes, France).

2.1.8. RANKL detection in Ewing's sarcoma experimental model by species-specific antibodies

Human or mouse RANKL was analyzed by ELISA on tumor and muscle lysatesand in serum of mice bearing TC-71 Ewing's sarcoma tumor. Tumor and muscle fragments were dry frozen and placed in 1 mL RLB 1 × (Promega) containing protease cocktail inhibitors 1 × (Roche), then ground using a Thurax Yellow^{line}DI 25 Basic Homogeneizer (IKA). The obtained solution is centrifuged 10 min at 12,000g at 4 °C and the supernatant is kept frozen at −20 °C. Samples were then analyzed for the production of murine or human RANKL using ELISA detection kits (R&D systems for mRANKL and Biomedica for hRANKL).

2.1.9. TRAIL detection by ELISA in Ewing's sarcoma experimental models

hTRAIL production was assessed by ELISA (R&D Systems, Abingdon, UK) in the supernatant of cultured Ewing sarcoma cells following the manufacturer's recommendations.

2.1.10. RANKL immuno-histochemistry in biopsies of Ewing's sarcoma patients

Two human biopsies from Ewing's sarcoma patients were analyzed for RANKL protein expression. Briefly, 3 μm sections were obtained from decalcified and paraffin embedded samples (from the anatomo-histo-pathology department of Nantes Hospital). After dewaxing and hydratation, antigen retrieval was performed with proteinase K solution (10 μg/mL in 1 × TBS–Tween 0.05%) at 37 °C. Then endogenous peroxydase activity was quenched with 3% H_2O_2 and unspecific sites were blocked with 5% goat serum, 1% BSA in 1 × TBS–Tween 0.05% at room temperature. Primary antibody (monoclonal mouse anti-human RANKL, R&D) was applied overnight at 4 °C. Immunodetection was performed using Streptavidin–Biotin complex followed by incubation with DAB Substrate-Chromogen (Dako) and counterstained with hematoxylin.

2.1.11. TRAIL immuno-histochemistry in biopsies of Ewing's sarcoma patients

Two human biopsies from Ewing's sarcoma patients were analyzed for RANKL protein expression. Briefly, 3 μm sections were obtained from decalcified and paraffin embedded samples (from the anatomo-histo-pathology department of Nantes Hospital). After dewaxing and hydratation, antigen retrieval was performed with 10 mM citrate buffer at 96 °C for 20 min. Following steps were performed as described above, except that primary antibody was goat anti-human TRAIL (R&D).

2.2. In vitro experiments

2.2.1. Ewing sarcoma

Ten human Ewing sarcoma cell lines were used. The A-673, TC-32, SK-ES-1, and RD-ES cell line were kindly provided by Dr. S. Burchill (Children's Hospital, Leeds, United Kingdom), the TC-71, SK-N-MC, STA-ET-1 and EW24 by Dr. O. Delattre (INSERM UMR830, Paris, France) and the BRZ from Dr. K. Scotlandi (Rizzoli Institute, Bologna, Italy). The A-673, TC-32 and RD-ES cell lines were cultured in DMEM (BioWhittaker), and TC-71, SK-ES-1, SK-N-MC and EW24 cell lines were cultured in RPMI (BioWhittaker) with 10% fetal bovine serum (FBS; Hyclone). In addition, TC-71 and STA-ET-1 cells require collagen for adherence and growing: before cell seeding, flasks were incubated 30 min with 50 μg/mL type I collagen (BD Biosciences) in 0.02 N acetic acid/PBS 1 ×.

2.2.2. Mesenchymal stem cells (MSC)

Bone marrow aspirates were obtained from patients during orthopedic surgical procedures after exposure of the iliac crest in the orthopedic department of Nantes University Hospital (Dr. J. Delécrin). Normal human MSC were then purified by centrifugation over Ficoll gradient (Sigma), 500,000 cells being seeded and cultivated in DMEM medium supplemented with 10% FBS. Adherent cells where then selected and cultivated with the same medium supplemented with bFGF (1 ng/mL, R&D systems). These cells are $CD105^+$, $CD90^+$, $CD45^-$ and $CD90^-$.

2.2.3. Cell proliferation and viability

Subconfluent cultures of Ewing's sarcoma cells in 96-well plates were treated for 72 h with increasing concentration (50, 100 and 200 ng/mL^{-1}) of hOPG (R&D systems). Cell viability was determined using the sodium 3′[1-(phenylaminocarbonyl)-3,4-tetrazolium]-bis(4-methoxy-6-nitro)benzene sulfonic acid hydrate (XTT) cell proliferation reagent assay kit (Roche). Cell viability was also assessed by trypan blue exclusion. The percentage of cells that exhibit intra-cytoplasmic trypan blue staining was determined using a Malassez counting chamber.

2.2.4. RANKL protein detection in Ewing's sarcoma cell lysates by western-blot

Total protein extracts in Laemmli buffer (62.5 mM Tris–HCl, pH 6.8, 2% SDS, 10% glycerol, 5% 2-mercaptoethanol, 0.001% bromophenol blue) were separated by SDS-polyacrylamide gel electrophoresis, and transferred to Immobilon-P membranes (Millipore). Membranes were immunoblotted with anti-human RANKL (1/200, Santa Cruz), or anti-β-actin (1/100, Sigma) antibodies. In both cases, secondary anti-rabbit antibody was used at 1/10,000 (Santa Cruz). Antibody binding was visualized with the enhanced chemiluminescence system (SuperSignal West Pico Chemiluminescent Substrate, ThermoSientific). For quantification, luminescence was detected with a Charge Couple Device (CCD) camera and analyzed using the GeneTools program (Syngene).

2.2.5. RANKL and TRAIL mRNA expression in ES cell lines by real time polymerase chain reaction

Total RNA was extracted using NucleoSpin®RNAII (Macherey Nagel) and used for first strand cDNA synthesis using ThermoScript RT-PCR System (Invitrogen). Real-time PCR was performed with a Chromo4 instrument (Biorad) using SYBR Green Supermix reagents (Biorad).

3. Results

3.1. RANKL is expressed by ES cells

The expression of RANKL was investigated at the mRNA and protein levels using respectively real time PCR and western-blot (and BioPlex) in the lysates of 10 human ES cell lines. RANKL mRNA expression was also compared to MSCs. Results presented in Fig. 1A showed that all Ewing's sarcoma cell lines studied express RANKL mRNA but at variable levels depending on the cell lines; RANKL seems to be more expressed in the SK-N-MC cell line, then SK-ES-1, EW24 and A-673, while some cell lines showed weak expression: TC-32, TC-71 or STA-ET-1. In comparison, MSC do not express RANKL. These results were partly confirmed at the

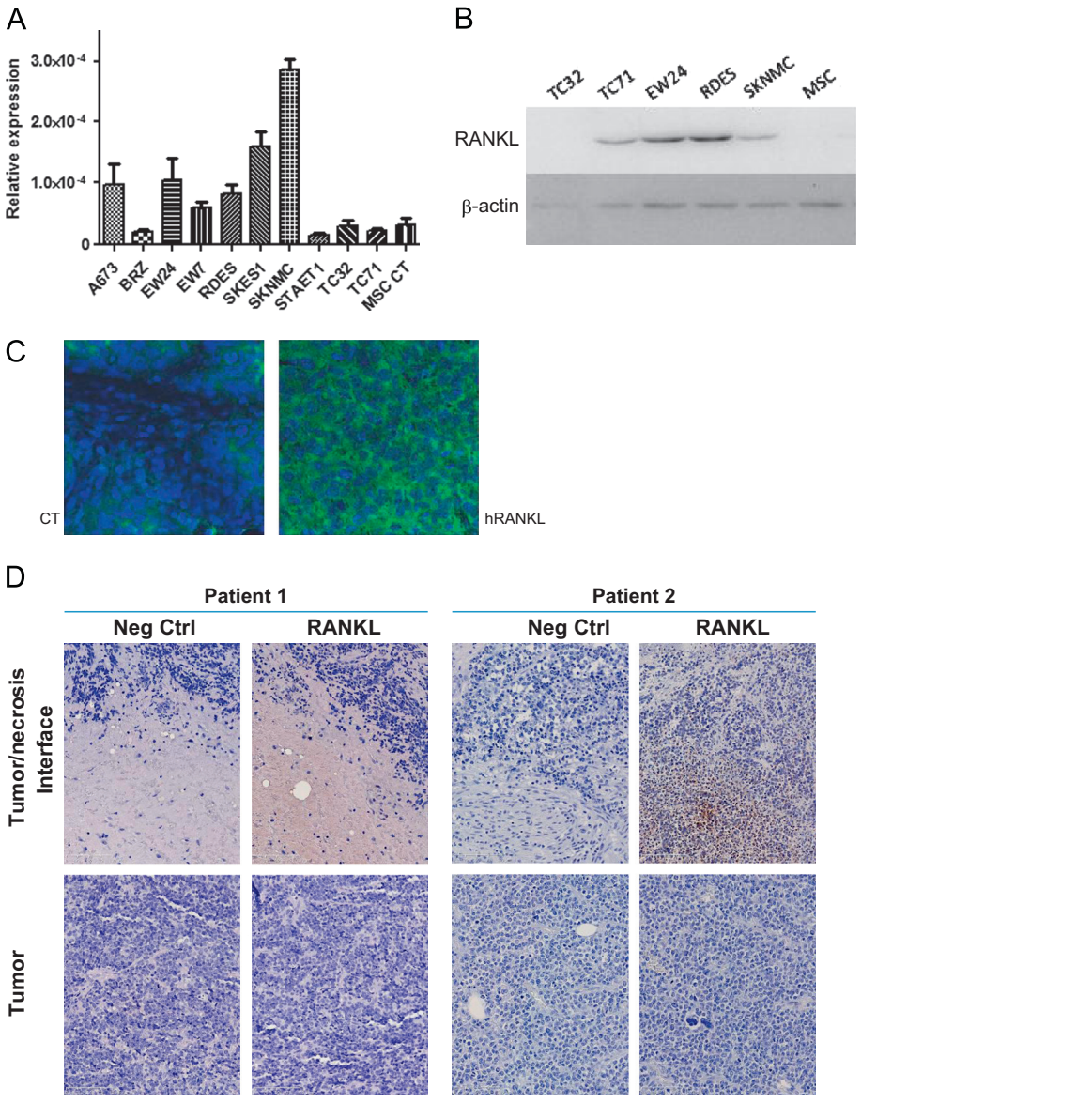

Fig. 1. Validation of the presence of RANKL in the Ewing's sarcoma tumor microenvironment. (A) The production of RANKL was analyzed at the mRNA level by real time PCR in 10 ES cell lines and compared to MSCs (see Section 2). (B) Basal RANKL protein expression is revealed by western-blot analysis in 5 ES cell lines and compared to human MSCs. (C) RANKL is detectable by immuno-fluorescence in tumors induced in mice by injection of 2×10^6 TC-71 ES cells (magnification 400 ×); (D) the presence of RANKL was evidenced in the biopsies of Ewing's sarcoma patient #2 (with relapsed aggressive tumor) while biopsy from patient 1 (good responder to chemotherapy) is negative (original magnification: 20 ×).

protein level by western-blot analysis: TC-71, EW24, RDES and SK-N-MC cell lines express RANKL, while TC-32 and MSC do not, confirming the results obtained at the mRNA level (Fig. 1B).

3.2. RANKL Is expressed in the ES tumor microenvironment

The expression of RANKL was then assessed in situ in tumor samples taken from A-673 human Ewing's sarcoma models (Fig. 1C). The immune staining was performed on 40-μm tumor sections by immuno-histofluorescence with antibodies targeting the human form of the cytokine (see Section 2). The staining protocol was designed to avoid cross reactions with the murine form of RANKL, by saturating the murine sites using goat anti-mouse Fab. A homogeneous expression of human RANKL was observed in sections of A-673 tumors as shown in Fig. 1C, similar results being obtained in another Ewing's Sarcoma model, in TC-71tumor sections (data not shown).

The human origin of RANKL production was confirmed in these models by ELISA test comparing the staining with antibodies specific of human or murine species. The human origin of RANKL was evidenced both at the systemic level in the serum (1.2 *versus* 0.05 ng/mL, $p < 0.001$ respectively) or in the muscle (1.4 *versus* 0.1 ng/mL, $p < 0.001$), but more importantly at the tumor level (4.4 *versus* 0.2 ng/mL, $p < 0.001$). Results presented in Table 1 clearly showed that RANKL detected in xenograft model of ES bearing mice is from human origin both at the local and systemic levels, with a more elevated amount found in the tumor itself.

3.3. RANKL is expressed in human biopsies of Ewing's sarcoma patients.

Immuno-histochemistry analysis of two Ewing's sarcoma patient biopsies show one positive and one negative staining for RANKL, depending on the clinical aggressiveness of the tumor (the RANKL-positive tumor corresponds to the more aggressive one which relapsed) (Fig. 1D). The positive staining was mostly evidenced around necrosis areas observed in the tumor. However, the cells producing RANKL seem to be the inflammatory cells or cells from the immune system rather than the tumor cells themselves.

Table 1
Origin of RANKL present in the tumor microenvironment. Tumor and muscle lysats, and serums of mice bearing Ewing's sarcoma were analyzed for the production of human and mouse RANKL using species-specific ELISA detection Kits. Results are expressed as ng/mL for serum detection and ng/mg of protein for detection on muscle or tumor lysat.

	Serum (ng/mL)	Tumor (ng/mg)	Muscle (ng/mg)
mRANKL	0.05	0.2	0.1
hRANKL	1.2***	4.4***	1.4***

*** $p < 0.001$.

3.4. Vaidation of hOPG transgene expression in mice

Orthotopic human ES models were induced in immuno-deficient mice as described in Section 2. The mice were treated with OPG by the injection of the F68/DNA complexes into the tibial anterior muscles in mice. hOPG transgene overexpression of was then validated by ELISA at both systemic (serum) and local (tumor) levels in mice treated with hOPG compared to mice receiving the mock pcDNA3.1 plasmid. Seven days after the first injection of the F68/DNA complex, the production of hOPG varied from 13.9 to 54.9 ng/mL in the serum of OPG-treated mice with a mean production of 29.2 ± 16 ng/mL, significantly higher than in the pcDNA3.1 group where no hOPG expression could be detected ($p < 0.001$, Fig. 2A). At the time of sacrifice, the hOPG concentration was also measured in the tumors. It reached a mean value of 17.8 ± 20.4 ng/mg in the hOPG treated group *versus* 2.9 ± 1.7 ng/mg in the pcDNA3.1 treated group ($p < 0.001$, Fig. 2B). The low level of hOPG detected in the tumors of pcDNA3.1-treated mice results probably from basal OPG production by the tumor cells themselves. No correlation could be established between the variability of OPG concentration and its therapeutic efficacy.

3.5. hOPG decreases ES tumor progression in vivo

A preventive protocol of non-viral gene transfer using the synthetic copolymer vector F68 from the Lutrol family was designed to determine the potential protective effect of hOPG1-194 on TC-71 ES tumor progression ($n=6$). The results obtained in the transplanted TC-71 model are representative of 4 other experiments performed in the Ewing's sarcoma TC-71 and A-673 models induced either by transplantation, or by intramuscular or intra-osseous injection of 2 millions corresponding cells. A decrease of the tumor incidence and a diminution of the tumor volume were observed in the group of OPG-treated mice whatever the model studied. For example at day 38 post-tumor cell injection, the mean tumor volume is diminished in hOPG-treated mice 1647.8 ± 1122 mm^3 as compared to pcDNA3.1 control mice $2658.9.5 \pm 1090.6$ mm^3 (Fig. 3A). Despite a clear tendency in all experiments, these results are statistically non-significant. However, they show that hOPG expression diminished the tumor incidence and progression

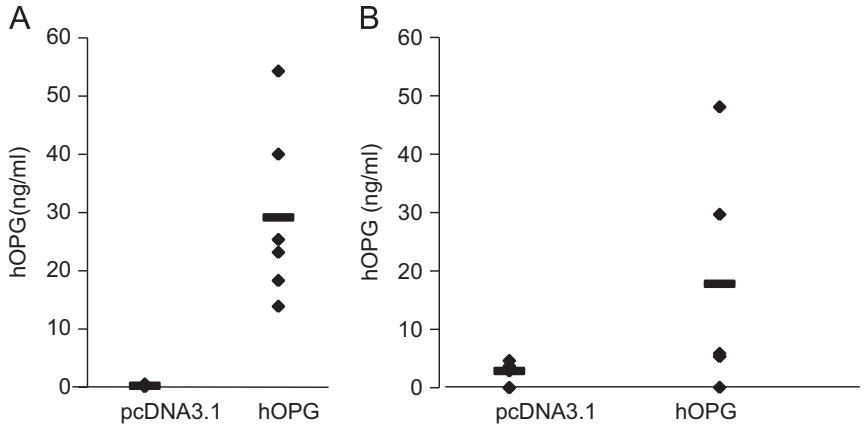

Fig. 2. *In vivo* validation of OPG transgene expression in mice. (A) hOPG transgene expression was assessed at the protein level by ELISA in the serum of mice, 7 days after the first DNA/Lutrol administration. (B) hOPG transgene expression was assessed at the protein level by ELISA in tumor fragments at the time of sacrifice.

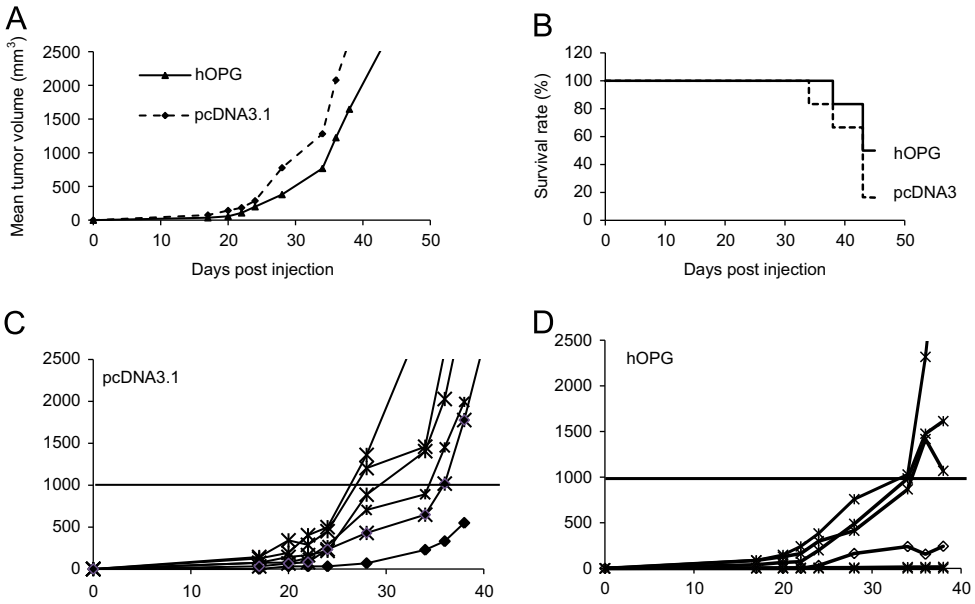

Fig. 3. OPG decreases tumor development and increases animal survival in EWS tumor models in mice. Tumors were induced on Nude mice by transplantation of a fragment of TC-71 tumor in close contact with the tibia as described in Section 2. Groups of 6 mice were assigned as pcDNA3.1 (empty pcDNA3.1 plasmid/F68 reagent) and hOPG (pcDNA3.1.3-hOPG1-194/F68 reagent). The F68/DNA formulations were administered through intrasmuscular injection into the 2 tibial anterior muscles weekly, beginning one week before tumor transplantation. (A) Mean tumor volume per group. (B) Overall survival for the 2 groups over a 42 days period. (C) Tumor volume evolution of individual mice.

and as a consequence, overall survival was increased in the hOPG group: 50% survival 43 days post-tumor implantation *versus* 16.3% in pcDNA3.1 (Fig. 3B). Moreover, when considering each animal individually 38 days after tumor transplantation, 5/6 mice had developed a primary tumor of at least 1000 mm^3 in the pcDNA3.1 group (Fig. 3C) *versus* only 2/6 in the hOPG-treated group (Fig. 3D).

3.6. OPG decreases tumor associated bone remodeling

Microscanner analysis previously revealed high levels of osteolytic lesions in the TC-71 ES model that was used in this study. Radiographs of the A-673 implanted mouse tibiae presented in Fig. 4A revealed a high bone remodeling, resulting in cortical destruction and intensive interactions between altered bone tissue and tumor cells, as compared with control mice (without tumor). Bone lesions appear to be slightly inhibited in mice treated with hOPG compared with mice treated with pcDNA3.1 (Fig. 4A). These results were confirmed and quantified by bone micro-architecture analysis, showing an intense bone remodeling in the pcDNA3.1 group while micro-architecture is preserved in hOPG treated animals (Fig. 4B). The specific bone volume of the trabeculae (BV/TV) was increased in hOPG treated mice as compared with the pcDNA3.1 group (respectively $43.5 \pm 5.4\%$ *versus* $40 \pm 4\%$, Fig. 4B). Overall, these results showed a slight anti-bone resorption effect of hOPG delivered by gene transfer using synthetic vectors in a preventive protocol developed in a mouse model of ES.

3.7. Recombinant soluble hOPG has no effect on ES cell proliferation in vitro

To determine whether the inhibitory effect of OPG observed *in vivo* could be due to direct effect on ES cell proliferation, TC-71 and A673 cells were treated during 72 h with increasing concentration of soluble recombinant hOPG (0–200 ng/mL). In both cell lines, no effect of hOPG on cell proliferation has been observed (Fig. 5A).

3.8. TRAIL is present in Ewing's sarcoma environment

In order to determine whether OPG inhibitory effects on RANKL activity could be partially modulated by TRAIL, another member of the TNF superfamily, we searched for TRAIL expression in the Ewing's sarcoma microenvironment. To this aim, we first analyze by ELISA test the capacity of 8 ES tumors induced by injection of 2 millions corresponding ES cells to produce TRAIL (Fig. 5B). Results clearly show that TRAIL can be detected in all the ES tumors studied, values varying from 2.2 to 10.3 pg/mg proteins in the cell lysate. As the ELISA test is human specific we can conclude that TRAIL is produce by the tumor itself. To determine whether TRAIL was produced directly by ES cells, its expression at the transcript level was analyzed by RT-qPCR in 10 ES cell lines and compared to normal human MSCs (Fig. 5C). The results showed that except for two cell lines (EW7 and SK-N-MC), ES cells do not express TRAIL.

In addition, TRAIL was detected by immuno-histochemistry in two biopsies of Ewing's sarcoma patients, but its expression is mainly associated with immune cells (Fig. 5D). This result suggests that OPG given as therapeutic molecule could bind in situ to both RANKL and TRAIL, and that TRAIL may interfere with OPG inhibitory effect on RANKL mediated pro-bone resorption activity in Ewing's sarcoma.

4. Discussion

Therapeutic interest has recently increased on bone tumor microenvironment as a new promising target for primary bone diseases. Even if tumor cells are still the first targets in cancer therapy, an increased number of data suggest that tumor cell proliferation in bone is highly dependent upon host cells from the bone microenvironment. Indeed, as evidenced for bone metastases, a vicious cycle between osteoclasts, bone stromal cells/osteoblasts and cancer cells have been hypothesized during the progression of primary bone tumors [11]. Tumor cells produce osteoclast activating factors such as Interleukin-6, TNF-α or PTH-rP

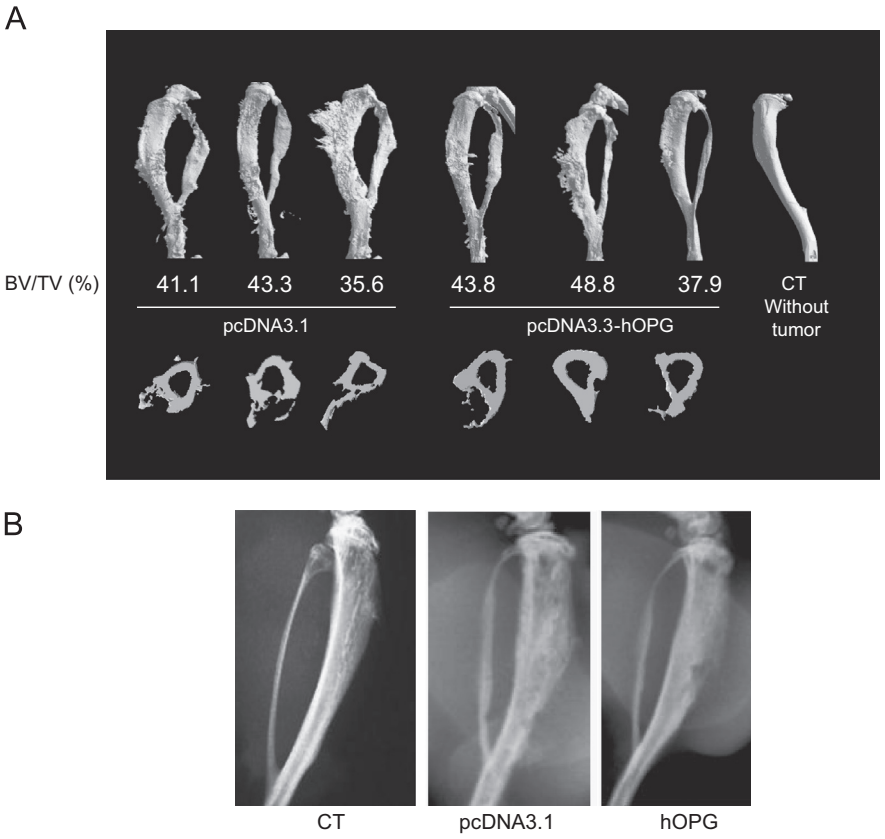

Fig. 4. Effect of OPG gene transfer on bone lesions associated with EWS progression in mice. (A) Tumor-associated osteolysis was analyzed by microCT at day 42 on 3 representative pcDNA3.1 mice and hOPG mice. The relative bone volume (BV/TV) is expressed as percent in each case. (B) Tumor-associated osteolysis analyzed by radiography at day 42 on pcDNA3.1 mice and hOPG mice.

that induce osteoclast differentiation and activation through the production of RANKL. When they resorb bone, osteoclasts enable the release of growth factors stored in the bone matrix (TGF-β, IGF-1, PDGF, *etc.*) that in turn activate tumor cell proliferation [11]. Accordingly, inhibition of osteoclast activity represents a promising approach to block the vicious cycle, inhibiting indirectly local cancer growth.

By inhibiting osteoclast activity, one possible option relies to bisphosphonates, the synthetic analogs of pyrophosphate that induce osteoclast apoptosis, decrease osteoclast activation and function by inhibition of the mevalonate pathway [32]. Such therapeutic tools have been studied in primary bone tumor models [33,34] and are even used in the French clinical trial OS2006 for pediatric and adult osteosarcoma patients. However, these molecules exhibit secondary events especially renal toxicity and osteonecrosis of the jaw, and may interfere with bone growth when administered to young patients [35].

Therefore, another promising way to block osteoclast activation is to target RANKL, the pivotal cytokine that mediate osteoclast differentiation and activation [36]. Beyond physiological conditions, increased expression of RANKL has been observed in osteolytic malignancies, such as breast cancer and multiple myeloma [37–39]. A previous study demonstrated that the RANKL/OPG ratio was significantly increased in patients suffering from severe osteolysis associated with tumor or not [19]. Therefore, therapeutic strategies that used its decoy receptor OPG have emerged in osteolytic bone tumor pathologies. As an example, OPG was shown to inhibit cancer cell migration and bone metastasis through inhibition of the RANKL-induced effects in RANK-expressing cells from tumor origin [40]. OPG was also shown to inhibit tumor-induced osteoclastogenesis and bone tumor growth in osteopetrotic mice [41], to reduce bone cancer pain by the blockade of the ongoing osteoclast activity [42], to decrease the number and area of radiographically evident lytic bone lesions in a model of mouse colon adenocarcinoma [21], to exhibit beneficial effects in experimental models of myeloma [20,43] and to inhibit osteolytic lesions associated with prostate cancer [44].

In the present study, mice developing Ewing's sarcoma models were treated by OPG administered by non-viral gene therapy. In a first step, we confirmed that RANKL was indeed a good therapeutic target in ES, by analyzing its expression both in patients and also in the ES models used in the present study. RANKL expression was indeed found in ES microenvironment in both cases, confirming the results previously published by Taylor et al. in patient biopsies [10]. Moreover, we demonstrate in the present study that ES cells are directly producing RANKL. The availability of a xenograft model of ES enabled us to discriminate from human or murine origin of RANKL production. The antibodies used were specific for each species and results clearly showed that the increased RANKL production in ES tumor model was due to direct synthesis by tumor cells. However, one interesting data is that some ES cell lines (such as TC-71) which express low levels of RANKL *in vitro* (Fig. 1A and B), show an elevated RANKL production when injected in the mouse and developing a tumor (Fig. 1C). Therefore, it suggests that during tumor development, the stroma may influence tumor cells to produce RANKL. These results constitute the rationale for the therapeutic use of OPG in ES.

A previous study from our group demonstrated that the truncated form of OPG (1-194) has greater activity than the complete form, given that proteoglycans present in the bone tumor microenvironment may bind to full length OPG, thereby limiting its bioavailability and bioactivity [31]. Therefore the truncated form of OPG was used in the present study. The transgene overexpression was confirmed both at the systemic

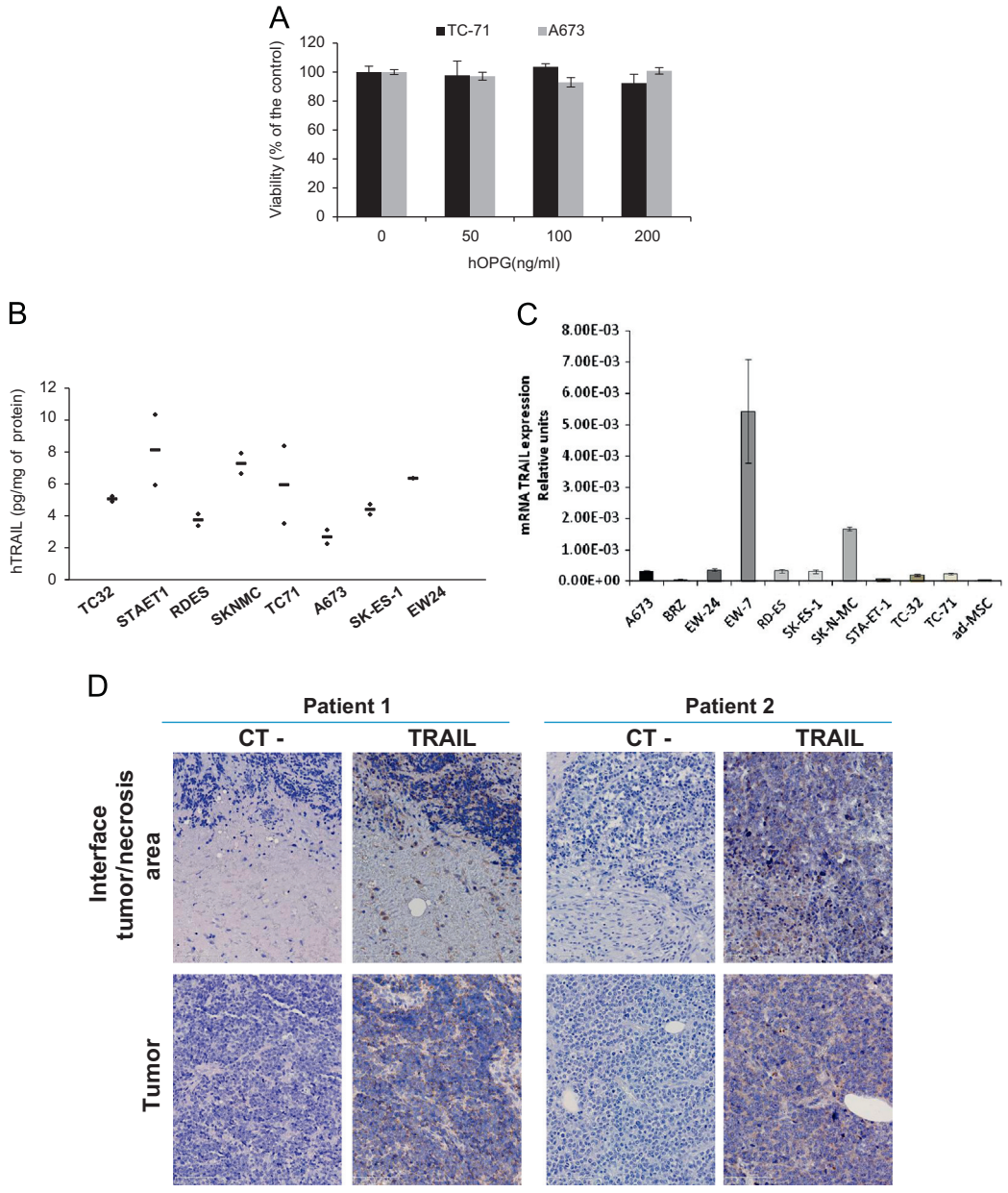

Fig. 5. Hypothesis on the OPG mechanisms of action in Ewing's sarcoma by binding TRAIL. (A) ES cells were cultured for 48 h in the presence of OPG. OPG has no direct effect on ES cell proliferation *in vitro*. (B) TRAIL is expressed in ES tumor models. Assays were realized on protein lysats obtained from fragments of tumors induced by intramuscular injection of human Ewing's sarcoma A-673 cells in nude mice, and normalized to respective protein levels (N=number of tumor samples analyzed). (C) The production of TRAIL was analyzed at the mRNA level by real time PCR in 10 ES cell lines and compared to human MSCs. (D) Two Ewing's sarcoma biopsies were analyzed for TRAIL immuno-staining (see Section 2) (original magnification 20 ×).

and local level of production. Microscanner analysis confirmed the OPG biological activity at the bone level, by prevention of osteolytic lesions and preservation of cortical bone structure at the tumor-bone interface. In addition, inhibition of tumor progression had been observed in all the series studied, both in models induced by transplantation of tumor fragments or by tumor cell injection. In all cases, the inhibition of the mean tumor volume was not significant (between 20% and 30% inhibition), probably due to the heterogeneity of the model but when considering each animal taken individually, there is a clear tendency to inhibition by OPG treatment either on incidence or progression levels. Because OPG has no direct effect on ES cell proliferation, OPG induced diminution of tumor growth could be explained by an indirect inhibitory effect on RANKL mediated bone resorption.

Several hypotheses can be proposed to explain why OPG has only weak effect on ES progression.

First, OPG is also able to bind another member of the TNF family, the TNF Related Apoptosis Inducing Ligand (TRAIL, TNFSF10)[45]. Several *in vitro* studies have even suggested that OPG could represent a protumoral factor for cancer cells, by inhibiting the pro-apoptosis activity of TRAIL [24–26]. This is why we searched for TRAIL expression and production in the ES microenvironment. We demonstrated that TRAIL is indeed detected in xenograft ES tumors induced by injection of corresponding human cells, but the ES cells themselves do not express TRAIL as evidenced in 8 ES cell lines out of 10. TRAIL protein level was also analyzed by immuno-histochemistry in human ES biopsies. Results showed that this cytokine is indeed present in the ES microenvironment, but mainly produced by immune cells rather than Es tumor cells. Therefore, TRAIL present in the microenvironment could interfere with OPG to modulate OPG inhibitory effect on RANKL activity [46]. In the same time, OPG expression was also

studied, both in the ES cell lines and in human ES biopsies. We showed that ES cell lines do not express OPG at all, this result being contradictory with those of Taylor et al. [10]. No OPG expression could be also observed in patient biopsies.

Therefore, another way to block RANKL activity should be proposed such as RANK-Fc or the humanized antibody anti-RANKL Denosumab [47]. However, because this fully humanized antibody cannot be used in preclinical studies in mice, we decided to test the soluble receptor OPG. Denosumab is able to specifically bind to RANKL blocking its activity, without any interference with other members of the TNF superfamily such as TRAIL or FasL [48]. At the clinical level, the use of Denosumab is already proposed for patients with malignancy associated osteolysis [49]. We could therefore propose to combine Denosumab with chemotherapy in the case of primary bone tumors, including Ewing's sarcoma.

Another hypothesis is that osteoclast activation is not only driven by RANKL, but also by other cytokines such as TNF-α or M-CSF (Macrophage-Colony Stimulating Factor). Indeed, previous data reported that macrophages present in the ES tumor stroma microenvironment could differentiate into osteoclasts in the presence of M-CSF and TNF-α [50]. In complement, the presence of both cytokines in the microenvironment of ES xenograft models was evidenced by immuno-fluorescence and ELISA (not shown). Therefore, a combined treatment could be proposed, associating an anti-RANKL strategy with anti-TNF and anti-M-CSF ones.

5. Conclusions

This study demonstrated that RANKL represents a good therapeutic target for ES patients, but OPG cannot be used per se because of its potential binding to TRAIL that may modulate its inhibitory activity towards RANKL. The potential involvement of two other cytokines that mediate osteoclast formation, i.e. TNF-α and M-CSF should be extensively studied as well in the Ewing sarcoma context.

Conflict of Interest statement

The authors declare that there are no conflicts of interest.

Acknowledgments

This work was supported by a grant from Novartis Pharma (Rueil-Malmaison, France), by the “Fédération Nationale Enfants et Santé”, the “Société Française de lutte contre les Cancers et les leucémies de l'Enfant et de l'Adolescent” and the “Institut National du Cancer” (Grant number R09018NN). The authors wish to thank G. Hamery and Y. Allain for their kind assistance at the animal facility care platform (Faculté de Médecine, Nantes, France) and J. Taurelle for his kind technical assistance (INSERM UMR957).

References

[1] Ewing J. Classics in Oncology. Diffuse Endothelioma of Bone. In: James Ewing (Ed.), Proceedings of the New York Pathological Society, 1921: CA; Cancer Journal for Clinicians 1972. 22: p. 95–8.
[2] Hense HW, Ahrens S, Paulussen M, Lehnert M, Jürgens H. Descriptive epidemiology of Ewing's tumor-analysis of German patients from (EI)CESS 1980–1997. Klinische Padiatrie 1999;211:271–5.
[3] Stiller CA, Bielack SS, Jundt G, Steliarova-Foucher E. Bone tumours in European children and adolescents, 1978-1997. Report from the Automated Childhood Cancer Information System project. European Journal of Cancer 2006;42:2124–35.
[4] Jaffe R, Santamaria M, Yunis EJ, et al. The neuroectodermal tumor of bone. American Journal of Surgical Pathology 1984;8:885–98.
[5] Folpe AL, Chand EM, Goldblum JR, Weiss SW. Expression of Fli-1, a nuclear transcription factor, distinguishes vascular neoplasms from potential mimics. American Journal of Surgical Pathology 2001;25:1061–6.
[6] May WA, Gishizky ML, Lessnick SL, et al. Ewing sarcoma 11;22 translocation produces a chimeric transcription factor that requires the DNA-binding domain encoded by FLI1 for transformation. Proceedings of the National Academy of Sciences USA 1993;90:5752–6.
[7] Nakatani F, Tanaka K, Sakimura R, et al. Identification of p21WAF1/CIP1 as a direct target of EWS-Fli1 oncogenic fusion protein. Journal of Biological Chemistry 2003;278:15105–15.
[8] Dauphinot L, De Oliveira C, Melot T, et al. Analysis of the expression of cell cycle regulators in Ewing cell lines: EWS-FLI-1 modulates p57KIP2 and c-Myc expression. Oncogene 2001;20:3258–65.
[9] Balamuth NJ, Womer RB. Ewing's sarcoma. Lancet Oncology 2010;11:184–92.
[10] Taylor R, Knowles HJ, Athanasou NA. Ewing sarcoma cells express RANKL and support osteoclastogenesis. Journal of Pathology 2011;225:195–202.
[11] Chirgwin JM, Guise TA. Molecular mechanisms of tumor-bone interactions in osteolytic metastases. Critical Reviews in Eukaryotic Gene Expression 2000;10:159–78.
[12] Simonet WS, Lacey DL, Dunstan CR, et al. Osteoprotegerin: a novel secreted protein involved in the regulation of bone density. Cell 1997;89:309–19.
[13] Wittrant Y, Théoleyre S, Chipoy C, et al. RANKL/RANK/OPG: new therapeutic targets in bone tumours and associated osteolysis. Biochimica et Biophysica Acta 2004;1704:49–57.
[14] Lacey DL, Timms E, Tan HL, et al. Osteoprotegerin ligand is a cytokine that regulates osteoclast differentiation and activation. Cell 1998;93:165–76.
[15] Theoleyre S, Wittrant Y, Tat SK, Fortun Y, Rédini F, Heymann D. The molecular triad OPG/RANK/RANKL: involvement in the orchestration of pathophysiological bone remodeling. Cytokine and Growth Factor Reviews 2004;15:457–75.
[16] Mizuno A, Amizuka N, Irie K, et al. Severe osteoporosis in mice lacking osteoclastogenesis inhibitory factor/osteoprotegerin. Biochemical and Biophysical Research Communications 1998;247:610–5.
[17] Bucay N, Sarosi I, Dunstan CR, et al. Osteoprotegerin-deficient mice develop early onset osteoporosis and arterial calcification. Genes and Development 1998;12:1260–8.
[18] Hofbauer LC, Neubauer A, Heufelder AE. Receptor activator of nuclear factor-kappaB ligand and osteoprotegerin: potential implications for the pathogenesis and treatment of malignant bone diseases. Cancer 2001;92:460–70.
[19] Grimaud E, Soubigou L, Couillaud S, et al. Receptor activator of nuclear factor kappaB ligand (RANKL)/osteoprotegerin (OPG) ratio is increased in severe osteolysis. American Journal of Pathology 2003;163:2021–31.
[20] Croucher PI, Shipman CM, Lippitt J, et al. Osteoprotegerin inhibits the development of osteolytic bone disease in multiple myeloma. Blood 2001;98:3534–40.
[21] Morony S, Capparelli C, Sarosi I, Lacey DL, Dunstan CR, Kostenuik PJ. Osteoprotegerin inhibits osteolysis and decreases skeletal tumor burden in syngeneic and nude mouse models of experimental bone metastasis. Cancer Research 2001;61:4432–6.
[22] Lamoureux F, Richard P, Wittrant Y, et al. Therapeutic relevance of osteoprotegerin gene therapy in osteosarcoma: blockade of the vicious cycle between tumor cell proliferation and bone resorption. Cancer Research 2007;67:7308–18.
[23] Rousseau J, Escriou V, Perrot P, et al. Advantages of bioluminescence imaging to follow siRNA or chemotherapeutic treatments in osteosarcoma preclinical models. Cancer Gene Therapy 2010;17:387–97.
[24] Emery JG, McDonnell P, Burke MB, et al. Osteoprotegerin is a receptor for the cytotoxic ligand TRAIL. Journal of Biological Chemistry 1998;273:14363–7.
[25] Holen I, Croucher PI, Hamdy FC, Eaton CL. Osteoprotegerin (OPG) is a survival factor for human prostate cancer cells. Cancer Research 2002;62:1619–23.
[26] Shipman CM, Croucher PI. Osteoprotegerin is a soluble decoy receptor for tumor necrosis factor-related apoptosis-inducing ligand/Apo2 ligand and can function as a paracrine survival factor for human myeloma cells. Cancer Research 2003;63:912–6.
[27] Pitard B, Pollard H, Agbulut O, et al. A nonionic amphiphile agent promotes gene delivery in vivo to skeletal and cardiac muscles. Human Gene Therapy 2002;13:1767–75.
[28] Pitard B, Bello-Roufai M, Lambert O, et al. Negatively charged self-assembling DNA/poloxamine nanospheres for in vivo gene transfer. Nucleic Acids Research 2004;32:e159.
[29] Desigaux L, Gourden C, Bello-Roufai M, et al. Nonionic amphiphilic block copolymers promote gene transfer to the lung. Human Gene Therapy 2005;16:821–9.
[30] Richard P, Bossard F, Desigaux L, Lanctin C, Bello-Roufai M, Pitard B. Amphiphilic block copolymers promote gene delivery in vivo to pathological skeletal muscles. Human Gene Therapy 2005;16:1318–24.
[31] Lamoureux F, Picarda G, Garrigue-Antar L, Baud'huin M, Trichet V, Vidal A, et al. Glycosaminoglycans as potential regulators of osteoprotegerin therapeutic activity in osteosarcoma. Cancer Research 2009;69:526–36.
[32] Rogers MJ, Gordon S, Benford HL, Coxon FP, Luckman SP, Monkkonen J, et al. Cellular and molecular mechanisms of action of bisphosphonates. Cancer 2000;88:2961–78.
[33] Heymann D, Ory B, Blanchard F, Heymann MF, Coipeau P, Charrier C, et al. Enhanced tumor regression and tissue repair when zoledronic acid is combined with ifosfamide in rat osteosarcoma. Bone 2005;37:74–86.

[34] Odri GA, Dumoucel S, Picarda G, Battaglia S, Lamoureux F, Corradini N, et al. Zoledronic acid as a new adjuvant therapeutic strategy for Ewing's sarcoma patients. Cancer Research 2010;70:7610–9.
[35] Battaglia S, Dumoucel S, Chesneau J, Heymann MF, Picarda G, Gouin F, et al. Impact of oncopediatric dosing regimen of zoledronic acid on bone growth: preclinical studies and case report of an osteosarcoma pediatric patient. Journal of Bone and Mineral Research 2011;26:2439–51.
[36] Hofbauer LC, Heufelder AE. Role of receptor activator of nuclear factor-kappaB ligand and osteoprotegerin in bone cell biology. Journal of Molecular Medicine 2001;79:243–53.
[37] Thomas RJ, Guise TA, Yin JJ, et al. Breast cancer cells interact with osteoblasts to support osteoclast formation. Endocrinology 1999;140:4451–8.
[38] Kitazawa S, Kitazawa R. RANK ligand is a prerequisite for cancer-associated osteolytic lesions. Journal of Pathology 2002;198:228–36.
[39] Wittrant Y, Theoleyre S, Chipoy C, et al. RANKL/RANK/OPG: new therapeutic targets in bone tumours and associated osteolysis. Biochimica et Biophysica Acta 2004;1704:49–57.
[40] Jones DH, Nakashima T, Sanchez OH, et al. Regulation of cancer cell migration and bone metastasis by RANKL. Nature 2006;440:692–6.
[41] Clohisy DR, Ramnaraine ML, Scully S, Qi M, Van HL, Lacey DL. Osteoprotegerin inhibits tumor-induced osteoclastogenesis and bone tumor growth in osteopetrotic mice. Journal of Orthopaedic Research 2000;18:967–76.
[42] Luger NM, Honore P, Sabino MA, et al. Osteoprotegerin diminishes advanced bone cancer pain. Cancer Research 2001;61:4038–47.
[43] Vanderkerken K, De Leenheer E, Shipman C, et al. Recombinant Osteoprotegerin decreases tumor burden and increases survival in a murine model of multiple myeloma. Cancer Research 2003;63:287–9.
[44] Yonou H, Kanomata N, Goya M, et al. Osteoprotegerin/osteoclastogenesis inhibitory factor decreases human prostate cancer burden in human adult bone implanted into nonobese diabetic/severe combined immunodeficient mice. Cancer Research 2003;63:2096–102.
[45] Emery JG, McDonnell P, Burke MB, Deen KC, Lyn S, Silverman C, et al. Osteoprotegerin is a receptor for the cytotoxic ligand TRAIL. Journal of Biological Chemistry 1998;273:14363–7.
[46] Lamoureux F, Moriceau G, Picarda G, Rousseau J, Trichet V, Rédini F. Regulation of osteoprotegerin pro- or anti-tumoral activity by bone tumor microenvironment. Biochimica et Biophysica Acta 2010;1805:17–24.
[47] Bekker PJ, Holloway DL, Rasmussen AS, Murphy R, Martin SW, Leese PT, et al. A single-dose placebo-controlled study of AMG 162, a fully human monoclonal antibody to RANKL, in postmenopausal women. Journal of Bone and Mineral Research 2004;19:1059–66.
[48] Kostenuik PJ, Nguyen HQ, McCabe J, Warmington KS, Kurahara C. Sun Net al. Denosumab, a fully human monoclonal antibody to RANKL, inhibits bone resorption and increases BMD in knock-in mice that express chimeric (murine/human) RANKL. Journal of Bone and Mineral Research 2009;24:182–95.
[49] Terpos E, Efstathiou E, Christoulas D, Roussou M, Katodritou E, Dimopoulos MA. RANKL inhibition: clinical implications for the management of patients with multiple myeloma and solid tumors with bone metastases. Expert Opinion on Biological Therapy 2009;9:465–79.
[50] Lau YS, Adamopoulos IE, Sabokbar A, Giele H, Gibbons CL, Athanasou NA. Cellular and humoral mechanisms of osteoclast formation in Ewing's sarcoma. British Journal of Cancer 2007;96:1716–22.